
LinkNet: Relational Embedding for Scene Graph

Sanghyun Woo**
EE, KAIST
Daejeon, Korea
shwoo93@kaist.ac.kr

Dahun Kim*
EE, KAIST
Daejeon, Korea
mcahny@kaist.ac.kr

Donghyeon Cho
EE, KAIST
Daejeon, Korea
cdh12242@gmail.com

In So Kweon
EE, KAIST
Daejeon, Korea
iskweon@kaist.ac.kr

Abstract

Objects and their relationships are critical contents for image understanding. A scene graph provides a structured description that captures these properties of an image. However, reasoning about the relationships between objects is very challenging and only a few recent works have attempted to solve the problem of generating a scene graph from an image. In this paper, we present a method that improves scene graph generation by explicitly modeling inter-dependency among the entire object instances. We design a simple and effective *relational embedding module* that enables our model to jointly represent connections among all related objects, rather than focus on an object in isolation. Our method significantly benefits main part of the scene graph generation task: relationship classification. Using it on top of a basic Faster R-CNN, our model achieves state-of-the-art results on the Visual Genome benchmark. We further push the performance by introducing *global context encoding module* and *geometrical layout encoding module*. We validate our final model, LinkNet, through extensive ablation studies, demonstrating its efficacy in scene graph generation.

1 Introduction

Current state-of-the-art recognition models have made significant progress in detecting individual objects in isolation [9, 20]. However, we are still far from reaching the goal of capturing the interactions and relationships between these objects. While objects are the core elements of an image, it is often the relationships that determine the global interpretation of the scene. The deeper understating of visual scene can be realized by building a structured representation which captures objects and their relationships jointly. Being able to extract such graph representations have been shown to benefit various high-level vision tasks such as image search [13], question answering [2], and 3D scene synthesis [29].

In this paper, we address *scene graph generation*, where the objective is to build a visually-grounded scene graph of a given image. In a scene graph, objects are represented as nodes and relationships between them as directed edges. In practice, a node is characterized by an object bounding box with a category label, and an edge is characterized by a predicate label that connects two nodes as a *subject-predicate-object* triplet. As such, a scene graph is able to model not only what objects are in the scene, but how they relate to each other.

*Both authors have equally contributed

The key challenge in this task is to reason about inter-object relationships. We hypothesize that explicitly modeling inter-dependency among the entire object instances can improve a model’s ability to infer their pairwise relationships. Therefore, we propose a simple and effective *relational embedding module* that enables our model to jointly represent connections among all related objects, rather than focus on an object in isolation. This significantly benefits main part of the scene graph generation task: relationship classification.

We further improve our network by introducing *global context encoding module* and *geometrical layout encoding module*. It is well known that fusing global and local information plays an important role in numerous visual tasks [8, 23, 39, 6, 40, 36]. Motivated by these works, we build a module that can provide contextual information. In particular, the module consists of global average pooling and binary sigmoid classifiers, and is trained for multi-label object classification. This encourages its intermediate features to represent all object categories present in an image, and supports our full model. Also, for the *geometrical layout encoding module*, we derive inspiration from the fact the most relationships in general are spatially regularized, implying that *subject-object* relative geometric layout can thus be a powerful cue for inferring the relationship in between. Our novel architecture results in our final model **LinkNet**, of which the overall architecture is illustrated in Fig. 1.

On the Visual Genome dataset, LinkNet obtains **state-of-the-art** results in scene graph generation tasks, revealing the efficacy of our approach. We visualize the weight matrices in relational embedding module and observe that inter-dependency between objects are indeed represented (see Fig. 2).

Contribution. Our main contribution is three-fold.

1. We propose a simple and effective *relational embedding module* in order to explicitly model inter-dependency among entire objects in an image. The *relational embedding module* improves the overall performance significantly.
2. In addition, we introduce *global context encoding module* and *geometrical layout encoding module* for more accurate scene graph generation.
3. The final network, LinkNet, has achieved new state-of-the-art performance in scene graph generation tasks on the large-scale benchmark [16]. Extensive ablation studies demonstrate the effectiveness of the proposed network.

2 Related Work

Relational Reasoning Relational reasoning has been explicitly modeled and adopted in neural networks. In the early days, most works attempted to apply neural networks to graphs, which are a natural structure for defining relations [11, 15, 24, 28, 1, 32]. Recently, the more efficient relational reasoning modules have been proposed [27, 30, 31]. Those can model dependency between the elements even with the non-graphical inputs, aggregating information from the feature embeddings at all pairs of positions in its input (e.g., pixels or words). The aggregation weights are automatically learned driven by the target task. While our work is connected to the previous works, an apparent distinction is that we consider object instances instead of pixels or words as our primitive elements. Since the objects have variations in scale/aspect ratio, we use ROI-align operation [9] to generate fixed 1D representations, easing the subsequent relation computations.

Moreover, relational reasoning of our model has a link to an attentional graph neural network. Similar to ours, Chen *et.al.* [4] uses a graph to encode spatial and semantic relations between regions and classes and passes information among them. To do so, they build a commonsense knowledge graph(*i.e.* adjacency matrix) from relationship annotations in the set. However, our approach does not require any external knowledge sources for the training. Instead, the proposed model generates soft-version of adjacency matrix(see Fig. 2) on-the-fly by capturing the inter-dependency among the entire object instances.

Relationship Detection The task of recognizing objects and the relationships has been investigated by numerous studies in a various form. This includes detection of human-object interactions [7, 3], localization of proposals from natural language expressions [12], or the more general tasks of visual relationship detection [17, 25, 38, 5, 19, 37, 34, 41] and scene graph generation [33, 18, 35, 22].

Among them, scene graph generation problem has recently drawn much attention. The challenging and open-ended nature of the task lends itself to a variety of diverse methods. For example: fixing

the structure of the graph, then refining node and edge labels using iterative message passing [33]; utilizing associative embedding to simultaneously identify nodes and edges of graph and piece them together [22]; extending the idea of the message passing from [33] with additional RPN in order to propose regions for captioning and solve tasks jointly [18]; staging the inference process in three-step based on the finding that object labels are highly predictive of relation labels [35];

In this work, we utilize relational embedding for scene graph generation. It utilizes a basic self-attention mechanism [30] within the aggregation weights. Compared to previous models [33, 18] that have been proposed to focus on message passing *between* nodes and edges, our model explicitly reasons about the relations *within* nodes and edges and predicts graph elements in multiple steps [35], such that features of a previous stage provides rich context to the next stage.

3 Proposed Approach

3.1 Problem Definition

A *scene graph* is a topological representation of a scene, which encodes object instances, corresponding object categories, and relationships between the objects. The task of *scene graph generation* is to construct a scene graph that best associates its nodes and edges with the objects and the relationships in an image, respectively.

Formally, the graph contains a node set \mathbf{V} and an edge set \mathbf{E} . Each node v_i is represented by a bounding box $v_i^{box} \in \mathbb{R}^4$, and a corresponding object class $v_i^{cls} \in \mathbf{C}_{obj}$. Each edge $e_{i \rightarrow j} \in \mathbf{C}_{rel}$ defines a relationship *predicate* between the *subject* node v_i and *object* node v_j . \mathbf{C}_{obj} is a set of object classes, \mathbf{C}_{rel} is a set of relationships. At the high level, the inference task is to classify objects, predict their bounding box coordinates, and classify pairwise relationship predicates between objects.

3.2 LinkNet

An overview of LinkNet is shown in Fig. 1. To generate a visually grounded scene graph, we need to start with an initial set of object bounding boxes, which can be obtained from ground-truth human annotation or algorithmically generated. Either cases are somewhat straightforward; In practice, we use a standard object detector, Faster R-CNN [26], as our bounding box model ($Pr(V^{box}|I)$). Given an image I , the detector predicts a set of region proposals V^{box} . For each proposal v_i^{box} , it also outputs a ROI-align feature vector \mathbf{f}_i^{RoI} and an object label distribution \mathbf{l}_i .

We build upon these initial object features \mathbf{f}_i^{RoI} , \mathbf{l}_i and design a novel scene graph generation network that consists of three modules. The first module is a *relational embedding module* that explicitly models inter-dependency among all the object instances. This significantly improves relationship classification ($Pr(E_{i \rightarrow j}|I, V^{box}, V^{cls})$). Second, *global context encoding module* provides our model with contextual information. Finally, the performance of predicate classification is further boosted by our *geometric layout encoding*.

In the following subsections, we will explain how each proposed modules are used in two main steps of scene graph generation: object classification, and relationship classification.

3.3 Object Classification

3.3.1 Object-Relational Embedding

For each region proposal, we construct a relation-based representation by utilizing the object features from the underlying RPN: the ROI-aligned feature $\mathbf{f}_i^{RoI} \in \mathbb{R}^{4096}$ and embedded object label distribution $\mathbf{K}_0 \mathbf{l}_i \in \mathbb{R}^{200}$. \mathbf{K}_0 denotes a parameter matrix that maps the distribution of predicted classes, \mathbf{l}_i , to \mathbb{R}^{200} . In practice, we use an additional image-level context features $\mathbf{c} \in \mathbb{R}^{512}$, so that each object proposal is finally represented as a concatenated vector $\mathbf{o}_i = (\mathbf{f}_i^{RoI}, \mathbf{K}_0 \mathbf{l}_i, \mathbf{c})$. We detail on the global context encoding in Sec. 3.3.2.

Then, for a given image, we can obtain N object proposal features $\mathbf{o}_i = 1, \dots, N$. Here, we consider *object-relational embedding* \mathbf{R} that computes the response for one object region \mathbf{o}_i by attending to the features from all N object regions. This is inspired by the recent works for relational reasoning [27, 30, 31]. Despite the connection, what makes our work distinctive is that we consider object-level

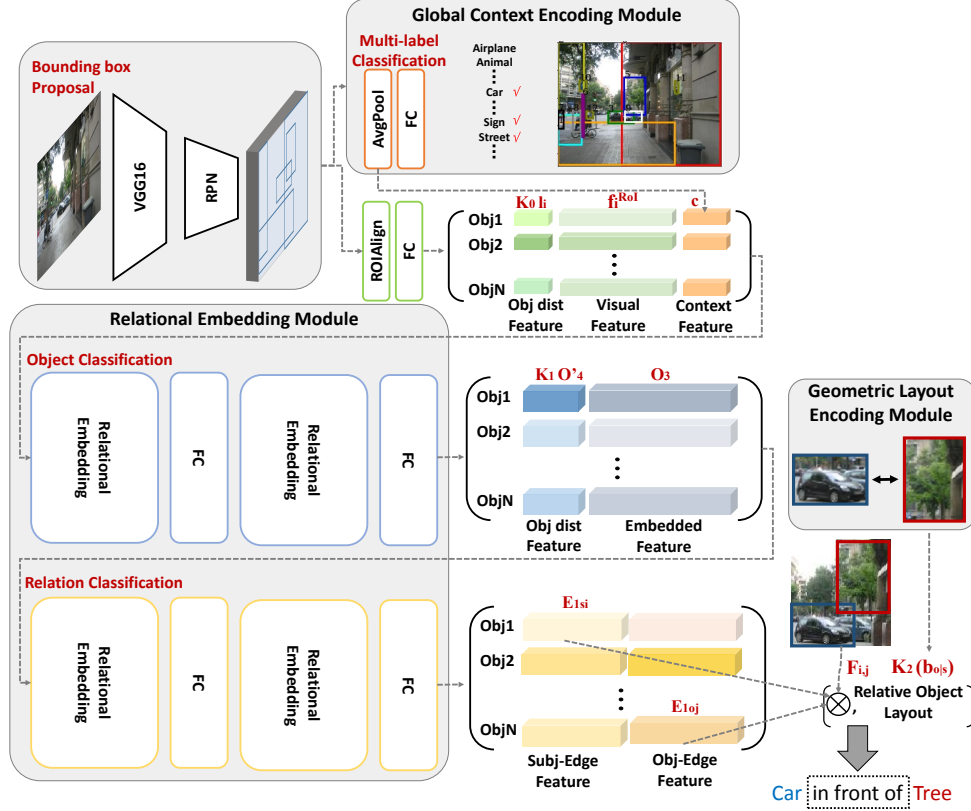


Figure 1: **The overview of LinkNet.** The model predicts graph in three steps: bounding box proposal, object classification, and relationship classification. The model consists of three modules: global context encoding module, relational embedding module, and geometric layout encoding module. Best viewed in color.

instances as our primitive elements, whereas the previous methods operate on pixels [27, 31] or words [30].

In practice, we stack all the object proposal features to build a matrix $\mathbf{O}_0 \in \mathbb{R}^{N \times 4808}$, from where we can compute a relational embedding matrix $\mathbf{R}_1 \in \mathbb{R}^{N \times N}$. Then, the relation-aware embedded features $\mathbf{O}_2 \in \mathbb{R}^{N \times 256}$ are computed as:

$$\mathbf{R}_1 = \text{softmax}((\mathbf{O}_0 \mathbf{W}_1)(\mathbf{O}_0 \mathbf{U}_1)^T) \in \mathbb{R}^{N \times N}, \quad (1)$$

$$\mathbf{O}_1 = \mathbf{O}_0 \oplus f_{c_0}((\mathbf{R}_1(\mathbf{O}_0 \mathbf{H}_1))) \in \mathbb{R}^{N \times 4808}, \quad (2)$$

$$\mathbf{O}_2 = f_{c_1}(\mathbf{O}_1) \in \mathbb{R}^{N \times 256}, \quad (3)$$

where \mathbf{W}_1 , \mathbf{U}_1 and \mathbf{H}_1 are parameter matrices that map the object features, \mathbf{O}_0 to $\mathbb{R}^{N \times \frac{4808}{r}}$, here we found setting hyper-parameter r as 2 produces best result from our experiment. The softmax operation is conducted in row-wise, constructing an embedding matrix. f_{c_0} and f_{c_1} are a parameter matrices that map its input feature of $\mathbb{R}^{N \times \frac{4808}{r}}$ to $\mathbb{R}^{N \times 4808}$, and $\mathbb{R}^{N \times 4808}$ to an embedding space $\mathbb{R}^{N \times 256}$, respectively. \oplus denotes a element-wise summation, allowing an efficient training overall due to residual learning mechanism [10]. The resulting feature \mathbf{O}_2 again goes through a similar relational embedding process, and is eventually embedded into object label distribution $\mathbf{O}_4 \in \mathbb{R}^{N \times C_{\text{obj}}}$ as:

$$\mathbf{R}_2 = \text{softmax}((\mathbf{O}_2 \mathbf{W}_2)(\mathbf{O}_2 \mathbf{U}_2)^T) \in \mathbb{R}^{N \times N}, \quad (4)$$

$$\mathbf{O}_3 = \mathbf{O}_2 \oplus f_{c_2}((\mathbf{R}_2(\mathbf{O}_2 \mathbf{H}_2))) \in \mathbb{R}^{N \times 256}, \quad (5)$$

$$\mathbf{O}_4 = f_{c_3}(\mathbf{O}_3) \in \mathbb{R}^{N \times C_{\text{obj}}}, \quad (6)$$

where \mathbf{W}_2 , \mathbf{U}_2 and \mathbf{H}_2 map the object features, \mathbf{O}_2 to $\mathbb{R}^{N \times \frac{256}{r}}$. The softmax operation is conducted in row-wise, same as above. f_{c_2} and f_{c_3} are another parameter matrices that map the intermediate features into $\mathbb{R}^{N \times \frac{256}{r}}$ to $\mathbb{R}^{N \times 256}$, and $\mathbb{R}^{N \times 256}$ to $\mathbb{R}^{N \times C_{obj}}$, respectively. Finally, the C_{obj} -way object classification $Pr(V^{cls}|I, V^{bbox})$ is optimized on the resulting feature \mathbf{O}_4 as:

$$\hat{V}^{cls} = \mathbf{O}_4, \quad (7)$$

$$\mathcal{L}_{obj_cls} = - \sum V^{cls} \log(\hat{V}^{cls}). \quad (8)$$

3.3.2 Global Context Encoding

Here we describe the *global context encoding module* in detail. This module is designed with the intuition that knowing contextual information in prior may help inferring individual objects in the scene.

In practice, we introduce an auxiliary task of multi-label classification, so that the intermediate features \mathbf{c} can encode all kinds of objects present in an image. More specifically, the *global context encoding* $\mathbf{c} \in \mathbb{R}^{512}$ is taken from an average pooling on the RPN image features ($\mathbb{R}^{512 \times H \times W}$), as shown in Fig. 1. This feature \mathbf{c} is concatenated with the initial image features ($\mathbf{f}_i, \mathbf{K}_0 \mathbf{l}_i$) as explained in Sec. 3.3.1, and supports scene graph generation performance as we will demonstrate in Sec. 4.2. After one parameter matrix, \mathbf{c} becomes multi-label distribution $\hat{\mathbf{M}} \in (0, 1)^{C_{obj}}$, and multi-label object classification (gce loss) is optimized on the ground-truth labels $\mathbf{M} \in [0, 1]^{C_{obj}}$ as:

$$\mathcal{L}_{gce} = - \sum_{c=1}^{C_{obj}} \mathbf{M}_c \log(\hat{\mathbf{M}}_c). \quad (9)$$

3.4 Relationship Classification

3.4.1 Edge-Relational Embedding

After the object classification, we further construct relation-based representations suitable for relationship classification. For this, we apply another sequence of *relational embedding modules*. In particular, the output of the previous *object-relational embedding module* $\mathbf{O}_4 \in \mathbb{R}^{N \times C_{obj}}$, and the intermediate feature $\mathbf{O}_3 \in \mathbb{R}^{N \times 256}$ are taken as inputs as:

$$\mathbf{O}'_4 = \text{argmax}(\mathbf{O}_4) \in \mathbb{R}^{N \times C_{obj}}, \quad (10)$$

$$\mathbf{E}_0 = (\mathbf{K}_1 \mathbf{O}'_4, \mathbf{O}_3) \in \mathbb{R}^{N \times (200+256)}, \quad (11)$$

where the argmax is conducted row-wise and produces an one-hot encoded vector \mathbf{O}'_4 which is then mapped into $\mathbb{R}^{N \times 200}$ by a parameter matrix \mathbf{K}_1 . Then, similar embedding operations as in Sec. 3.3.1 are applied on \mathbf{E}_0 , resulting in embedded features $\mathbf{E}_1 \in \mathbb{R}^{N \times 8192}$, where the half of the channels(4096) refers to *subject* edge features and its counterpart refers to *object* (see Fig. 1).

For each possible $N^2 - N$ edges, say between \mathbf{v}_i and \mathbf{v}_j , we compute the probability the edge will have label $e_{i \rightarrow j}$ (including the background). We operate on \mathbf{E}_1 and an embedded features from the union region of i -th and j -th object regions, $\mathbf{F} = \{ \mathbf{f}_{i,j} \mid i \in (1, 2, \dots, N), j \in (1, 2, \dots, N), j \neq i \} \in \mathbb{R}^{N(N-1) \times 4096}$ as:

$$\mathbf{G}_{0ij} = (\mathbf{E}_{1_{si}} \otimes \mathbf{E}_{1_{oj}} \otimes \mathbf{F}_{ij}) \in \mathbb{R}^{4096}, \quad (12)$$

$$\mathbf{G}_1 = (\mathbf{G}_0, \mathbf{K}_2(\mathbf{b}_{o|s})) \in \mathbb{R}^{N(N-1) \times (4096+128)}, \quad (13)$$

$$\mathbf{G}_2 = f_{c_4}(\mathbf{G}_1) \in \mathbb{R}^{N(N-1) \times C_{rel}}. \quad (14)$$

We combine *subject* edge features, *object* edge features and union image representations by low-rank outer product [14]. $\mathbf{b}_{o|s}$ denotes relative geometric layout which is detailed in Sec. 3.4.2. It is embedded into $\mathbb{R}^{N(N-1) \times 128}$ by a parameter matrix \mathbf{K}_2 . A parameter matrix f_{c_4} maps the intermediate features $\mathbf{G}_1 \in \mathbb{R}^{N(N-1) \times 4224}$ into $\mathbf{G}_2 \in \mathbb{R}^{N(N-1) \times C_{rel}}$.

Methods	Predicate Classification			Scene Graph Classification			Scene Graph Detection		
	R@20	R@50	R@100	R@20	R@50	R@100	R@20	R@50	R@100
VRD [21]		27.9	35.0		11.8	14.1		0.3	0.5
MESSAGE PASSING [33]		44.8	53.0		21.7	24.4		3.4	4.2
ASSOC EMBED [22]	47.9	54.1	55.4	18.2	21.8	22.6	6.5	8.1	8.2
MOTIFNET [35]	58.5	65.2	67.1	32.9	35.8	36.5	21.4	27.2	30.3
LinkNet	61.8	67.0	68.5	38.3	41	41.7	22.3	27.4	30.1

Table 1: The table shows our model achieves state-of-the-art result in Visual Genome benchmark [16]. Note that the **Predicate Classification** and **Scene Graph Classification** tasks assume exactly same perfect detector across the methods, and evaluate how well the each models predict object labels and their relations, while **Scene Graph Detection** task takes a customized pre-trained detector and performs subsequent tasks.

Finally, the \mathbf{C}_{rel} -way relationship classification $Pr(E_{i \rightarrow j} | I, V^{bbox}, V^{cls})$ is optimized on the resulting feature \mathbf{G}_2 as:

$$E_{i \rightarrow j} = \mathbf{G}_2, \quad (15)$$

$$\mathcal{L}_{rel_cls} = - \sum_{i=1}^N \sum_{j \neq i} E_{i \rightarrow j} \log(\hat{E}_{i \rightarrow j}). \quad (16)$$

3.4.2 Geometric Layout Encoding

We hypothesize that relative geometry between the *subject* and *object* is a powerful cue for inferring the relationship between them. Indeed, many *predicates* have straightforward correlation with the *subject-object* relative geometry, whether they are geometric (e.g., 'behind'), possessive (e.g., 'has'), or semantic (e.g., 'riding').

To exploit this cue, we encode the relative location and scale information as :

$$\mathbf{b}_{o|s} = (\frac{\mathbf{x}_o - \mathbf{x}_s}{\mathbf{w}_s}, \frac{\mathbf{y}_o - \mathbf{y}_s}{\mathbf{h}_s}, \log(\frac{\mathbf{w}_o}{\mathbf{w}_s}), \log(\frac{\mathbf{h}_o}{\mathbf{h}_s})), \quad (17)$$

where $\mathbf{x}, \mathbf{y}, \mathbf{w}$, and \mathbf{h} denote the x, y -coordinates, width, and height of the object proposal, and the subscripts o and s denote *object* and *subject*, respectively. we embed $\mathbf{b}_{o|s}$ to a feature in $\mathbb{R}^{N \times 128}$ and concatenate this with the *subject-object* features as in Eq. (13).

3.5 Loss

The whole network can be trained in an end-to-end manner, allowing the network to predict object bounding boxes, object categories, and relationship categories sequentially (see Fig. 1). Our loss function for an image is defined as:

$$\mathcal{L}_{final} = \mathcal{L}_{obj_cls} + \lambda_1 \mathcal{L}_{rel_cls} + \lambda_2 \mathcal{L}_{gce}. \quad (18)$$

By default, we set λ_1 and λ_2 as 1, and thus all the terms are equally weighted.

4 Experiments

We conduct experiments on Visual Genome benchmark [16].

4.1 Quantitative Evaluation

Since the current work in scene graph generation is largely inconsistent in terms of data splitting and evaluation, we compared against papers [21, 33, 22, 35] that followed the original work [33]. The experimental results are summarized in Table. 1.

The LinkNet achieves new **state-of-the-art** results in Visual Genome benchmark [16], demonstrating its efficacy in identifying and associating objects. For the scene graph classification and predicate classification tasks, our model outperforms the strong baseline [35] by a large margin. Note that predicate classification and scene graph classification tasks assume the same perfect detector across the methods, whereas scene graph detection task depends on a customized pre-trained detector.

Independent Variables	Value	Scene Graph Classification		
		R@20	R@50	R@100
Number of REM	1	37.7	40.4	41
	ours(2)	38.3	41	41.7
	3	37.9	40.6	41.3
	4	38	40.7	41.4
Reduction ratio (r)	1	38	40.9	41.6
	ours(2)	38.3	41	41.7
	4	38.2	41	41.6
	8	37.7	40.5	41.2

a Experiments on hyperparams.

b Design-choices in constructing E_0 .

Table 2: **(a)** includes experiments for the optimal value for the two hyper parameters; **(b)** includes experiments to verify the effective design choices of constructing E_0

Exp	REM	Proposed		Row-wise		Similarity		Scene Graph Classification			predicate	R@100	
		GLEM	GCEM	Softmax	Sigmoid	Dot prod	Eucl	R@20	R@50	R@100		w. GLEM	w.o GLEM
1	✓			✓		✓		37.4	40.0	40.8	using	0.269	0.000
2	✓	✓		✓		✓		37.9	40.4	41.2	carrying	0.246	0.118
3	✓		✓	✓		✓		38.0	40.6	41.3	riding	0.249	0.138
4	✓	✓			✓	✓		37.7	40.3	41	behind	0.341	0.287
5	✓		✓	✓			✓	37.2	40.0	40.7	at	0.072	0.040
6	✓	✓	✓	✓			✓	37.9	40.7	41.4	in front of	0.094	0.069
Ours	✓	✓	✓	✓		✓		38.3	41	41.7	has	0.495	0.473
											wearing	0.488	0.468
											on	0.570	0.551
											sitting on	0.088	0.070

Table 3: The **left table** shows ablation studies on the final model. The **right table** summarizes top-10 predicates with highest recall increase in scene graph classification with the use of geometric layout encoding module. **REM**, **GLEM**, **GCEM** denotes Relational Embedding Module, Geometric Layout Encoding Module, and Global Context Encoding Moudle respectively.

4.2 Ablation Study

In order to evaluate the effectiveness of our model, we conduct four ablation studies based on the scene graph classification task as follows. Results of the ablation studies are summarized in Table. 2 and Table. 3.

Experiments on hyperparameters The first row of Table. 2a shows the results of *more relational embedding modules*. We argue that multiple modules can perform multi-hop communication. Messages between all the objects can be effectively propagated, which is hard to do via standard models. However, too many modules can arise optimization difficulty. Our model with two REMs achieved the best results. In second row of Table. 2a, we compare performance with four different *reduction ratios*. The reduction ratio determines the number of channels in the module, which enables us to control the capacity and overhead of the module. The reduction ratio 2 achieves the best accuracy, even though the reduction ratio 1 allows higher model capacity. We see this as an over-fitting since the training losses converged in both cases. Overall, the performance drops off smoothly across the reduction ratio, demonstrating that our approach is robust to it.

Design-choices in constructing E_0 Here we construct an input(E_0) of edge-relational embedding module by combining an object class representation(O'_4) and a global contextual representation(O_3). The operations are inspired by the recent work [35] that contextual information is critical for the relationship classification of an objects. To do so, we turn O_4 of object label probabilities into one-hot vectors via an argmax operation(committed to a specific object class label) and we concatenate it with an output(O_3) which passed through the relational embedding module(contextualized representation). As shown in the Table. 2b, we empirically confirm that both operations contribute to the performance boost.

The effectiveness of proposed modules. We perform an ablation study to validate our modules in the network, which are relation embedding module, geometric layout encoding module, and global context encoding module. We remove each module to verify the effectiveness of utilizing all the proposed modules. As shown in Exp 1, 2, 3, and Ours, we can clearly see the performance improvement when we use all the modules jointly. This shows that each module plays a critical role together in inferring object labels and their relationships. Note that **Exp 1** already achieves



Figure 2: **Visualization of relational embedding matrices.** For each example, the first row shows ground-truth object regions. The left and right column of the second row show ground-truth relations (binary, 1 if present, 0 otherwise), and the weights of our relational embedding matrix, respectively. Note how the relational embedding relates the objects with a real connection, compared to those in none-relationship.

state-of-the-art result, showing that utilizing *relational embedding module* is crucial while the other modules further boost performance.

The effectiveness of GLEM. We conduct additional analysis to see how the network performs with the use of *geometric layout encoding module*. We select top-10 predicates with highest recall increase in scene graph classification task. As shown in right side of Table. 3, we empirically confirm that the recall value of geometrically related predicates are significantly increased, such as *using*, *carrying*, *riding*. In other words, predicting predicates which have clear *subject-object* relative geometry, was helped by the module.

Row-wise operation methods. In this experiment, we conduct an ablation study to compare row-wise operation methods in relational embedding matrix: softmax and sigmoid; As we can see in Exp 4 and Ours, softmax operation which imposes competition along the row dimension performs better, implying that explicit attention mechanism [30] which emphasizes or suppresses relations between objects helps to build more informative embedding matrix.

Relation computation methods. In this experiment, we investigate two commonly used relation computation methods: dot product and euclidean distance. As shown in Exp 1 and 5, we observe that dot-product produces slightly better result, indicating that relational embedding behavior is crucial for the improvement while it is less sensitive to computation methods. Meanwhile, Exp 5 and 6 shows that even we use euclidean distance method, *geometric layout encoding module* and *global context encoding module* further improves the overall performance, again showing the efficacy of the introduced modules.

4.3 Qualitative Evaluation

Visualization of relational embedding matrix We visualize our relational embedding of our network in Fig. 2. For each example, the bottom-left is the ground-truth binary triangular matrix where its entry is filled as: $(i, j | i < j) = 1$ only if there is a non-background relationship(in any direction) between the i -th and j -th instances, and 0 otherwise. The bottom-right is the trained weights of an intermediate relational embedding matrix (Eq. (4)), folded into a triangular form. The results show that our relational embedding represents inter-dependency among all object instances, being consistent with the ground-truth relationships. To illustrate, in the first example, the ground-truth matrix refers to the relationships between the 'man'(1) and his body parts(2,3); and the 'mountain'(0) and the 'rocks'(4,5,6,7), which are also reasonably captured in our relational embedding matrix. Note that our model infers relationship correctly even there exists missing ground-truths such as cell(7,0) due to sparsity of annotations in Visual Genome dataset. Indeed, our *relational embedding module*

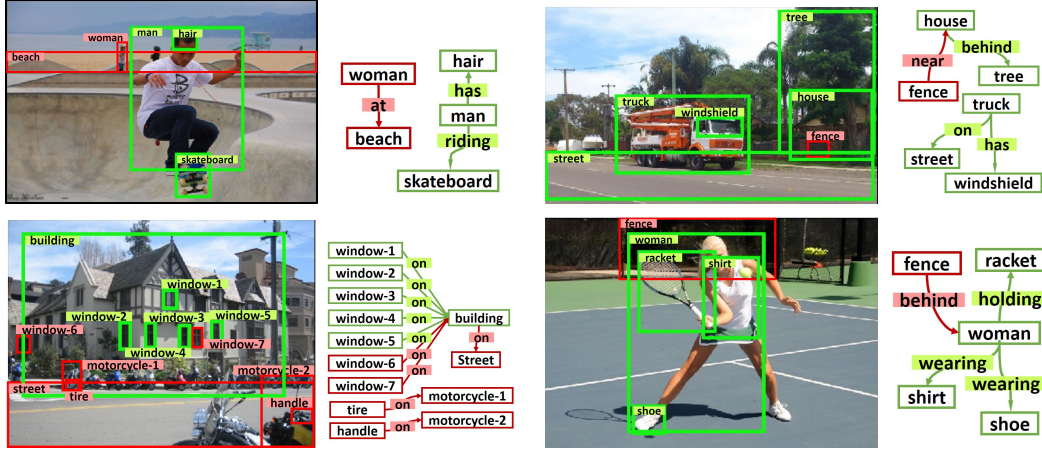


Figure 3: **Qualitative examples of our scene graph detection results.** Green boxes and edges are correct predictions, and red boxes and edges are false negatives.

plays a key role in scene graph generation, leading our model to outperform previous state-of-the-art methods.

Scene graph detection Qualitative examples of scene graph detection of our model are shown in Fig. 3. We observe that our model properly induces scene graph from a raw image.

5 Conclusion

We addressed the problem of generating a scene graph from an image. Our model captures global interactions of objects effectively by proposed *relational embedding module*. Using it on top of basic Faster R-CNN system significantly improves the quality of node and edge predictions, achieving state-of-the-art result. We further push the performance by introducing *global context encoding module* and *geometric layout encoding module*, constructing a LinkNet. Through extensive ablation experiments, we demonstrate the efficacy of our approach. Moreover, we visualize relational embedding matrix and show that relations are properly captured and utilized. We hope LinkNet become a generic framework for scene graph generation problem.

Acknowledgements This research is supported by the Study on Deep Visual Understanding funded by the Samsung Electronics Co., Ltd (Samsung Research)

References

- [1] Peter Battaglia, Razvan Pascanu, Matthew Lai, Danilo Jimenez Rezende, et al. Interaction networks for learning about objects, relations and physics. In *Proc. of Neural Information Processing Systems (NIPS)*, 2016.
- [2] Angel Chang, Manolis Savva, and Christopher D Manning. Learning spatial knowledge for text to 3d scene generation. In *Proc. of Conference on Empirical Methods in Natural Language Processing (EMNLP)*, 2014.
- [3] Yu-Wei Chao, Yunfan Liu, Xieyang Liu, Huayi Zeng, and Jia Deng. Learning to detect human-object interactions. *arXiv preprint arXiv:1702.05448*, 2017.
- [4] Xinlei Chen, Li-Jia Li, Li Fei-Fei, and Abhinav Gupta. Iterative visual reasoning beyond convolutions. *arXiv preprint arXiv:1803.11189*, 2018.
- [5] Bo Dai, Yuqi Zhang, and Dahua Lin. Detecting visual relationships with deep relational networks. In *Proc. of Computer Vision and Pattern Recognition (CVPR)*, 2017.
- [6] Pedro F Felzenszwalb, Ross B Girshick, David McAllester, and Deva Ramanan. Object detection with discriminatively trained part-based models. *IEEE transactions on pattern analysis and machine intelligence*, 32(9):1627–1645, 2010.
- [7] Georgia Gkioxari, Ross Girshick, Piotr Dollár, and Kaiming He. Detecting and recognizing human-object interactions. In *Proc. of Computer Vision and Pattern Recognition (CVPR)*, 2018.
- [8] Jinwei Gu, Jie Zhou, and Chunyu Yang. Fingerprint recognition by combining global structure and local cues. *IEEE Transactions on Image Processing*, 15(7):1952–1964, 2006.
- [9] Kaiming He, Georgia Gkioxari, Piotr Dollár, and Ross Girshick. Mask r-cnn. In *Proc. of Int’l Conf. on Computer Vision (ICCV)*, 2017.
- [10] Kaiming He, Xiangyu Zhang, Shaoqing Ren, and Jian Sun. Deep residual learning for image recognition. In *Proc. of Computer Vision and Pattern Recognition (CVPR)*, 2016.
- [11] Mikael Henaff, Joan Bruna, and Yann LeCun. Deep convolutional networks on graph-structured data. *arXiv preprint arXiv:1506.05163*, 2015.
- [12] Ronghang Hu, Marcus Rohrbach, Jacob Andreas, Trevor Darrell, and Kate Saenko. Modeling relationships in referential expressions with compositional modular networks. In *Proc. of Computer Vision and Pattern Recognition (CVPR)*, 2017.
- [13] Justin Johnson, Ranjay Krishna, Michael Stark, Li-Jia Li, David Shamma, Michael Bernstein, and Li Fei-Fei. Image retrieval using scene graphs. In *Proc. of Computer Vision and Pattern Recognition (CVPR)*, 2015.
- [14] Jin-Hwa Kim, Kyoung-Woon On, Woosang Lim, Jeonghee Kim, Jung-Woo Ha, and Byoung-Tak Zhang. Hadamard product for low-rank bilinear pooling. In *Proc. of Int’l Conf. on Learning Representations (ICLR)*, 2017.
- [15] Thomas N Kipf and Max Welling. Semi-supervised classification with graph convolutional networks. In *Proc. of Int’l Conf. on Learning Representations (ICLR)*, 2017.
- [16] Ranjay Krishna, Yuke Zhu, Oliver Groth, Justin Johnson, Kenji Hata, Joshua Kravitz, Stephanie Chen, Yannis Kalantidis, Li-Jia Li, David A Shamma, et al. Visual genome: Connecting language and vision using crowdsourced dense image annotations. *International Journal of Computer Vision*, 123(1):32–73, 2017.
- [17] Yikang Li, Wanli Ouyang, Xiaogang Wang, and Xiao’Ou Tang. Vip-cnn: Visual phrase guided convolutional neural network. In *Proc. of Computer Vision and Pattern Recognition (CVPR)*, 2017.
- [18] Yikang Li, Wanli Ouyang, Bolei Zhou, Kun Wang, and Xiaogang Wang. Scene graph generation from objects, phrases and region captions. In *Proc. of Int’l Conf. on Computer Vision (ICCV)*, 2017.
- [19] Xiaodan Liang, Lisa Lee, and Eric P Xing. Deep variation-structured reinforcement learning for visual relationship and attribute detection. In *Proc. of Computer Vision and Pattern Recognition (CVPR)*, 2017.
- [20] Tsung-Yi Lin, Priya Goyal, Ross Girshick, Kaiming He, and Piotr Dollár. Focal loss for dense object detection. In *Proc. of Int’l Conf. on Computer Vision (ICCV)*, 2017.
- [21] Cewu Lu, Ranjay Krishna, Michael Bernstein, and Li Fei-Fei. Visual relationship detection with language priors. In *Proc. of European Conf. on Computer Vision (ECCV)*, 2016.
- [22] Alejandro Newell and Jia Deng. Pixels to graphs by associative embedding. In *Proc. of Neural Information Processing Systems (NIPS)*, 2017.
- [23] Wei-Zhi Nie, An-An Liu, Zan Gao, and Yu-Ting Su. Clique-graph matching by preserving global & local structure. In *Proc. of Computer Vision and Pattern Recognition (CVPR)*. IEEE, 2015.

- [24] Mathias Niepert, Mohamed Ahmed, and Konstantin Kutzkov. Learning convolutional neural networks for graphs. In *Proc. of Int'l Conf. on Machine Learning (ICML)*, 2016.
- [25] Bryan A Plummer, Arun Mallya, Christopher M Cervantes, Julia Hockenmaier, and Svetlana Lazebnik. Phrase localization and visual relationship detection with comprehensive image-language cues. In *Proc. of Computer Vision and Pattern Recognition (CVPR)*, 2017.
- [26] Shaoqing Ren, Kaiming He, Ross Girshick, and Jian Sun. Faster r-cnn: Towards real-time object detection with region proposal networks. In *Proc. of Neural Information Processing Systems (NIPS)*, 2015.
- [27] Adam Santoro, David Raposo, David G Barrett, Mateusz Malinowski, Razvan Pascanu, Peter Battaglia, and Tim Lillicrap. A simple neural network module for relational reasoning. In *Proc. of Neural Information Processing Systems (NIPS)*, 2017.
- [28] Franco Scarselli, Marco Gori, Ah Chung Tsoi, Markus Hagenbuchner, and Gabriele Monfardini. The graph neural network model. *IEEE Transactions on Neural Networks*, 20(1):61–80, 2009.
- [29] Damien Teney, Lingqiao Liu, and Anton van den Hengel. Graph-structured representations for visual question answering. *CoRR, abs/1609.05600*, 3, 2016.
- [30] Ashish Vaswani, Noam Shazeer, Niki Parmar, Jakob Uszkoreit, Llion Jones, Aidan N Gomez, Łukasz Kaiser, and Illia Polosukhin. Attention is all you need. In *Proc. of Neural Information Processing Systems (NIPS)*, 2017.
- [31] Xiaolong Wang, Ross Girshick, Abhinav Gupta, and Kaiming He. Non-local neural networks. In *Proc. of Computer Vision and Pattern Recognition (CVPR)*, 2018.
- [32] Nicholas Watters, Andrea Tacchetti, Theophane Weber, Razvan Pascanu, Peter Battaglia, and Daniel Zoran. Visual interaction networks. In *Proc. of Neural Information Processing Systems (NIPS)*, 2017.
- [33] Danfei Xu, Yuke Zhu, Christopher B Choy, and Li Fei-Fei. Scene graph generation by iterative message passing. In *Proc. of Computer Vision and Pattern Recognition (CVPR)*, 2017.
- [34] Ruichi Yu, Ang Li, Vlad I Morariu, and Larry S Davis. Visual relationship detection with internal and external linguistic knowledge distillation. In *Proc. of Int'l Conf. on Computer Vision (ICCV)*, 2017.
- [35] Rowan Zellers, Mark Yatskar, Sam Thomson, and Yejin Choi. Neural motifs: Scene graph parsing with global context. In *Proc. of Computer Vision and Pattern Recognition (CVPR)*, 2018.
- [36] Hang Zhang, Kristin Dana, Jianping Shi, Zhongyue Zhang, Xiaogang Wang, Amrith Tyagi, and Amit Agrawal. Context encoding for semantic segmentation. In *Proc. of Computer Vision and Pattern Recognition (CVPR)*, 2018.
- [37] Hanwang Zhang, Zawlin Kyaw, Shih-Fu Chang, and Tat-Seng Chua. Visual translation embedding network for visual relation detection. In *Proc. of Computer Vision and Pattern Recognition (CVPR)*, 2017.
- [38] Hanwang Zhang, Zawlin Kyaw, Jinyang Yu, and Shih-Fu Chang. Ppr-fcn: weakly supervised visual relation detection via parallel pairwise r-fcn. In *Proc. of Int'l Conf. on Computer Vision (ICCV)*, 2017.
- [39] Hengshuang Zhao, Jianping Shi, Xiaojuan Qi, Xiaogang Wang, and Jiaya Jia. Pyramid scene parsing network. In *Proc. of Computer Vision and Pattern Recognition (CVPR)*, 2017.
- [40] Yousong Zhu, Chaoyang Zhao, Jinqiao Wang, Xu Zhao, Yi Wu, and Hanqing Lu. Couplenet: Coupling global structure with local parts for object detection. In *Proc. of Int'l Conf. on Computer Vision (ICCV)*, 2017.
- [41] Bohan Zhuang, Lingqiao Liu, Chunhua Shen, and Ian Reid. Towards context-aware interaction recognition. In *Proc. of Int'l Conf. on Computer Vision (ICCV)*, 2017.